

AN ALMA CONSTRAINT ON THE GSC 6214-210 B CIRCUM-SUBSTELLAR ACCRETION DISK MASS

BRENDAN P. BOWLER^{1,6}, SEAN M. ANDREWS², ADAM L. KRAUS³, MICHAEL J. IRELAND⁴, GREGORY HERCZEG⁵,
LUCA RICCI², JOHN CARPENTER¹, AND MICHAEL E. BROWN¹¹ California Institute of Technology, 1200 E. California Boulevard, Pasadena, CA 91125, USA; bpbowler@caltech.edu² Harvard-Smithsonian Center for Astrophysics, 60 Garden Street, Cambridge, MA 02138, USA³ Department of Astronomy, The University of Texas at Austin, Austin, TX 78712, USA⁴ Research School of Astronomy & Astrophysics, Australian National University, Canberra, ACT 2611, Australia⁵ Kavli Institute for Astronomy and Astrophysics, Peking University, Yi He Yuan Lu 5, Haidian Qu, Beijing 100871, China

Received 2015 April 3; accepted 2015 May 6; published 2015 May 28

ABSTRACT

We present Atacama Large Millimeter/submillimeter Array (ALMA) observations of GSC 6214-210 A and B, a solar-mass member of the 5–10 Myr Upper Scorpius association with a $15 \pm 2 M_{\text{Jup}}$ companion orbiting at ≈ 330 AU ($2/2$). Previous photometry and spectroscopy spanning $0.3\text{--}5 \mu\text{m}$ revealed optical and thermal excess as well as strong H α and Pa β emission originating from a circum-substellar accretion disk around GSC 6214-210 B, making it the lowest-mass companion with unambiguous evidence of a subdisk. Despite ALMA’s unprecedented sensitivity and angular resolution, neither component was detected in our $880 \mu\text{m}$ (341 GHz) continuum observations down to a 3σ limit of 0.22 mJy/beam. The corresponding constraints on the dust mass and total mass are $<0.15 M_{\oplus}$ and $<0.05 M_{\text{Jup}}$, respectively, or $<0.003\%$ and $<0.3\%$ of the mass of GSC 6214-210 B itself assuming a 100:1 gas-to-dust ratio and characteristic dust temperature of 10–20 K. If the host star possesses a putative circum-stellar disk then at most it is a meager 0.0015% of the primary mass, implying that giant planet formation has certainly ceased in this system. Considering these limits and its current accretion rate, GSC 6214-210 B appears to be at the end stages of assembly and is not expected to gain any appreciable mass over the next few megayears.

Key words: accretion, accretion disks – brown dwarfs – stars: individual (GSC 6214-210)

1. INTRODUCTION

Giant planets are common products of protoplanetary disk evolution but many of the details of their formation remain obscure and untested. Core accretion is the dominant formation channel at small separations of $\lesssim 10$ AU (Pollack et al. 1996; Alibert et al. 2005), while disk instability (Boss 1997) and turbulent fragmentation (Bate 2009) operate on wider orbits at tens to hundreds of AU. In these outer regions ($\sim 10\text{--}300$ AU), high-contrast direct imaging surveys are revealing that the tail end of the substellar companion mass function is likely to be continuous (Brandt et al. 2014), extends down to at least $\approx 5 M_{\text{Jup}}$ (Kuzuhara et al. 2013; Rameau et al. 2013), and overlaps with the most massive planets like HR 8799 bcde (Marois et al. 2008, 2010) and β Pic b (Lagrange et al. 2009), which probably formed in massive protoplanetary disks.

In all formation scenarios, giant planets accrete most of their mass from circum-planetary disks, which naturally form around protoplanets in an analogous way to circumstellar disks around protostars (Vorobyov & Basu 2010; Ward & Canup 2010). Circum-planetary disks regulate angular momentum transport and accretion as protoplanets grow, ultimately determining the final masses of giant planets (Quillen & Trilling 1998; Lubow et al. 1999; Canup & Ward 2002; Zhu 2015). At the earliest stages of giant planet assembly ($\lesssim 3$ Myr), accretion shocks from circum-planetary disks onto protoplanets help to define planets’ initial entropy levels and which evolutionary pathways (hot, warm, or cold start models) they will follow (Marley et al. 2007). Moreover, the formation, bulk composition, and orbits of moons are also governed by properties of circum-planetary disks (Heller et al. 2014). Physically, these disks are

expected to be quite thick ($h/r > 0.2$), possess little flaring compared to their circum-stellar analogs, and be tidally truncated to $\sim 1/3 R_{\text{Hill}}$ from gravitational influence of the host star (Ayliffe & Bate 2009; Martin & Lubow 2011; Shabram & Boley 2013).

This epoch of planet growth is challenging to study directly because of the small angular resolution and high contrasts required. The possible discovery of extended thermal excess emission from the candidate protoplanets LkCa 15 b (Kraus & Ireland 2012) and HD 100546 b (Quanz et al. 2013) may represent the first direct detections of circum-planetary disks, though the masses and immediate environments of these embedded companions are still poorly constrained (Isella et al. 2014). The remnants of circum-planetary disks are evident from the prograde, regular satellites orbiting gas giants in our solar system as well as the (possibly transient) ring systems surrounding Saturn, the substellar companion 1SWASP J140747.93–394542.6 (Mamajek et al. 2012; Kenworthy & Mamajek 2015), and perhaps Fomalhaut b (Kalas et al. 2008).

Over the past decade a population of young ($\lesssim 10$ Myr) planetary-mass companions on ultra-wide orbits (> 100 AU) has been uncovered with direct imaging (see Table 1 of Bowler et al. 2014). Many of these possess their own accretion disks, offering unique opportunities to study the structure, diversity, and evolution of circum-planetary disks. Recently Kraus et al. (2015) presented 1.3 mm Atacama Large Millimeter/submillimeter Array (ALMA) continuum observations of FW Tau C, a young (≈ 2 Myr), wide-separation (330 AU) companion with a possible mass as low as $6\text{--}14 M_{\text{Jup}}$ (Kraus et al. 2014). The clear detection at millimeter wavelengths implies a dust mass of $1\text{--}2 M_{\oplus}$, sufficient to form a system of rocky moons. However, the high veiling and possible edge-on architecture of the this

⁶ Caltech Joint Center for Planetary Astronomy Fellow.

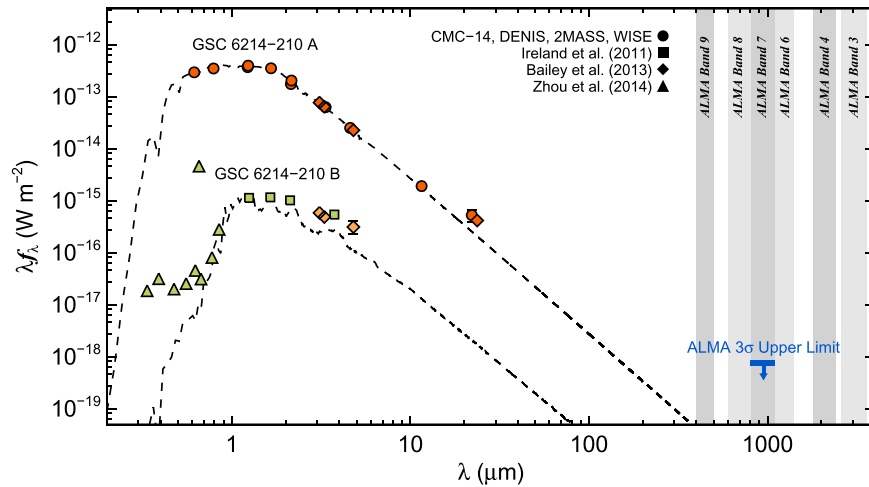


Figure 1. Spectral energy distributions of GSC 6214-210 A (red) and B (green). GSC 6214-210 B exhibits optical and thermal excess along with extraordinarily strong H α emission. The unresolved pair shows slight excess beyond 12 μm that could originate from the circum-substellar disk around GSC 6214-210 B and/or a low-mass disk around the primary. Our ALMA 880 μm 3 σ upper limit (blue) rules out substantial disks from both components. Photometry for the primary are from CMC-14 (r'), DENIS (IJK), 2MASS (JHK), *WISE* (3.4, 4.6, 12, and 22 μm), and *Spitzer*/MIPS (24 μm ; Bailey et al. 2013). Note that the 3.1, 3.3 μm , and M' photometry of GSC 6214-210 A from Bailey et al. (2013) are inferred rather than independently measured. Photometry for GSC 6214-210 B are from Ireland et al. (2011; $JHKL'$), Bailey et al. (2013; 3.1, 3.3 μm , M'), and Zhou et al. (2014; 0.33–0.85 μm). The BT-Settl 4200 K/4.0 dex and 2400 K/4.5 dex models (dashed lines; Allard et al. 2010) scaled to the J -band photometry are shown for comparison.

accretion disk makes the mass of FW Tau C highly uncertain and possibly well above the planetary regime (Bowler et al. 2014).

Here we present ALMA 880 μm continuum observations of GSC 6214-210 B, a $\approx 15 M_{\text{Jup}}$ companion orbiting the young (5–10 Myr) Sun-like star GSC 6214-210 A in Upper Scorpius (USco) at 330 AU. With a mass at the deuterium-burning limit and abundant evidence of ongoing accretion, GSC 6214-210 B is the lowest-mass companion with a circum-substellar disk currently known. ALMA’s unprecedented sensitivity and angular resolution at sub-millimeter and millimeter wavelengths presents a unique opportunity to characterize a sub-disk at the boundary between the brown dwarf and planetary mass regimes. Additionally, ALMA observations provide important contextual information about any circum-stellar disk surrounding GSC 6214-210 A, or lack thereof in case of a non-detection.

2. THE GSC 6214-210 AB SYSTEM

GSC 6214-210 is a well-established member of the USco star-forming region (Preibisch et al. 1998; Ireland et al. 2011; Luhman & Mamajek 2012). Low-mass evolutionary models point to an age of ≈ 5 Myr for this complex, though more recent turn-off ages suggest it is somewhat older (≈ 10 Myr; Pecaut et al. 2012). Based on its spectral type ($K5 \pm 1$) and modest reddening ($A_V \sim 0.6$ mag), evolutionary models imply a mass of $0.9 \pm 0.1 M_{\odot}$ for the primary (Baraffe et al. 1998; Bowler et al. 2011). GSC 6214-210 is an evolved Class III object with no signs of a substantial disk out to 12 μm .

The low-mass companion to GSC 6214-210 was first identified at 2'2 (330 AU) from Keck/AO imaging by Kraus et al. (2008) and confirmed to be comoving with the primary by Ireland et al. (2011). Evolutionary models imply a mass of $15 \pm 2 M_{\text{Jup}}$ from its age (5–10 Myr) and luminosity ($\log L_{\text{bol}}/L_{\odot} = -3.1 \pm 0.1$ dex). Bowler et al. (2011, 2014) found a near-infrared spectral type of $M9.5 \pm 1$ for GSC 6214-210 B as well as strong Pa β emission at 1.282 μm ($\text{EW} = -11.2 \text{ \AA}$), indicating vigorous accretion from a circum-substellar disk.

Recently, 1.0–2.4 μm spectroscopy by Lachapelle et al. (2015) also revealed Pa β emission as well as weak Br γ emission at 2.166 μm . Optical imaging with *Hubble Space Telescope* by Zhou et al. (2014) uncovered extraordinarily strong H α emission ($\text{EW} \sim -1600 \text{ \AA}$) and continuum excess shortward of $\sim 6000 \text{ \AA}$, corresponding to an accretion rate of $\dot{M} \sim 10^{-10.8} M_{\odot} \text{ yr}^{-1}$. 3–5 μm imaging by Ireland et al. (2011) and Bailey et al. (2013) supports the presence of a warm disk from thermal excess emission above the photospheric level. Unresolved 22 μm photometry of GSC 6214-210 AB from *WISE* and 24 μm photometry from *Spitzer* (Bailey et al. 2013) reveal a slight (but significant) excess, which could be from an evolved disk around the primary and/or a massive disk surrounding the companion (Figure 1). Synthesized W4-band photometry of the 4200 K/4.0 dex and 2400 K/4.5 dex BT-Settl models in Figure 1 implies a range of flux densities for the companion between $9.92 \times 10^{-20} \text{ W m}^{-2} \mu\text{m}^{-1}$ (or $2.19 \times 10^{-18} \text{ W m}^{-2}$ at 22 μm , assuming no excess) to $1.2 \pm 0.6 \times 10^{-17} \text{ W m}^{-2} \mu\text{m}^{-1}$ (or $2.6 \pm 1.3 \times 10^{-16} \text{ W m}^{-2}$ at 22 μm , assuming the excess is entirely attributed to the companion).

3. ALMA OBSERVATIONS

GSC 6214-210 AB ($\alpha = 16:21:54.67$, $\delta = -20:43:09.2$) was observed with ALMA in Band 7 at 880 μm (341 GHz) during Cycle 2 Early Science operations on UT 2014 June 30. Thirty-one 12m antennas targeted this system with the dual-polarization setup in four spectral windows centered at 334.0, 336.0, 346.0, and 347.8 GHz. The 346.0 GHz window encompasses the CO ($J = 3-2$) line and was sampled in 1920 channels each with a width of 0.98 MHz (frequency division correlator mode), while the other three continuum windows comprised 128 channels at 15.6 MHz each (time division correlator mode). The total on-source integration time was 11.6 minutes and the total effective bandwidth was 7.7 GHz. The maximum array baseline reached 650 m, resulting in a synthesized beam FWHM of $0''.32 \times 0''.41$ at a position angle of $96:3$ and a field of view spanning $18'' \times 18''$.

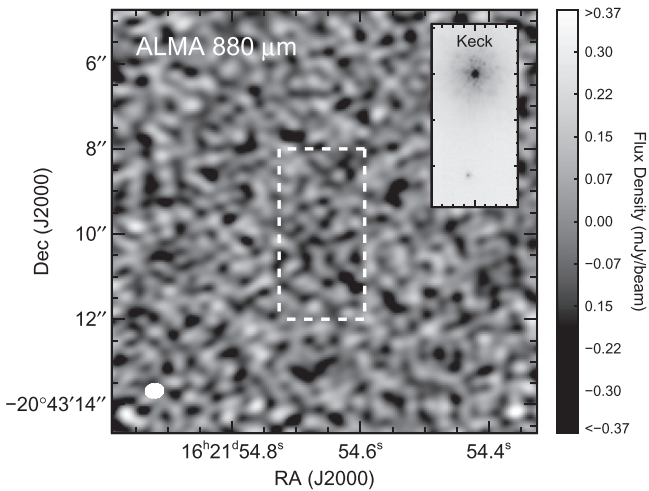


Figure 2. ALMA 880 μm continuum image centered on GSC 6214-210 AB. The inset shows a $2'' \times 4''$ K' -band Keck/NIRC2 adaptive optics image of the pair from Ireland et al. (2011). The same region is depicted as a dashed box in the ALMA image. Neither component is detected with a 3σ upper limit of 0.22 mJy (assuming a point source). The field of view is $10'' \times 10''$ and the $0.7'' \times 0.4''$ beam FWHM is shown as a white ellipse in the bottom left corner. The image has been corrected for the nonuniform sensitivity of the primary beam across the field of view, and the color stretch spans $\pm 5\sigma$ (± 0.37 mJy/beam).

The visibility data reduction and image reconstruction were carried out with CASA version 4.2.2. The primary calibrator was the nearby quasar QSO J1625-2527, which was targeted intermittently during the science observations. No line emission was detected in the 346.0 GHz data so this window was incorporated with the continuum regions to create an averaged continuum image. No detections are present above the background rms level of 0.074 mJy/beam as measured in the central $3\frac{1}{2}'' \times 3\frac{1}{2}''$ region. Finally, the continuum image was corrected for the non-uniform sensitivity across the field of view by dividing by the primary beam response. The result is shown in Figure 2.

4. RESULTS

There is no significant emission above the background level (0.074 mJy/beam rms) at the location of GSC 6214-210 A or its companion, implying a 3σ upper limit of 0.22 mJy (assuming a point source). With a spatial resolution of $\approx 0.4''$, both components would be easily separated in our observations. Assuming the continuum emission is optically thin, an upper limit on the dust mass (M_{dust}) can be derived from our ALMA flux density constraint, the distance to the system (145 pc), a characteristic isothermal disk temperature (T_C), and a dust opacity (κ_ν) following Hildebrand (1983). For consistency with previous work we use the frequency-dependent dust opacity relationship $\kappa_\nu = 10(\nu/10^{12} \text{ Hz}) \text{ cm}^2 \text{ g}^{-1}$ from Beckwith et al. (1990). At 880 μm , the dust opacity $\kappa_{880 \mu\text{m}}$ is $3.4 \text{ cm}^2 \text{ g}^{-1}$.

Following Andrews et al. (2013), we adopt the dust temperature-stellar luminosity relationship $T_C = 25 (L/L_\odot)^{1/4}$ for the primary GSC 6214-210 A. This yields $T_C = 20$ K using the luminosity of $\log L/L_{\text{Bol}} = -0.42 \pm 0.08$ dex from Bowler et al. (2011). Heating of GSC 6214-210 B's outer disk is probably dominated by GSC 6214-210 A or diffuse interstellar radiation rather than irradiation by GSC 6214-210 B itself. We therefore assume a dust temperature between 10 and 20 K for

GSC 6214-210 B, which is within the range of disk midplane temperatures for isolated brown dwarfs (Ricci et al. 2014).

The 3σ dust mass upper limit is $<0.05 M_\oplus$ (3.9 lunar masses) for the primary and $<0.05\text{--}0.15 M_\oplus$ (3.9–12.6 lunar masses) for the companion. For a gas-to-dust ratio of 100, this implies putative disk masses of $<5 M_\oplus$ for GSC 6214-210 A and $<15 M_\oplus$ for B. These results are most sensitive to the characteristic disk temperature, dipping to $0.03 M_\oplus$ (2.8 lunar masses) of dust for a slightly warmer temperature of 25 K, and increasing to $0.9 M_\oplus$ (76 lunar masses) for a temperature of 5 K. The lower limit on dust temperature is set by the diffuse interstellar radiation field and cosmic rays, which even for dense starless cloud cores that are shielded from external radiation is only about 10 K. So although our dust mass upper limit is highly sensitive to the dust temperature, we consider the dust mass of $\sim 0.15 M_\oplus$ set by a $T_C = 10$ K to be a fairly strict upper limit on sub-millimeter-sized particles and smaller. The total disk mass also depends on the grain size distribution, which is especially important for an older, presumably evolved system like this. If planetesimals have formed then they can also lock up a significant amount of solid mass, though there is an upper limit to this storage since fragmenting collisions would grind them back down to approximately millimeter sizes that would be detectable with these ALMA observations. Moreover, since the gas-to-dust ratio in protoplanetary disks is generally highly uncertain and evolves over time, the total disk masses in this work are approximate at best.

5. DISCUSSION

Our deep 880 μm upper limit implies that GSC 6214-210 B's disk has a low mass ($\lesssim 0.05 M_{\text{Jup}}$) and lacks a significant amount of cold dust in its outer regions. This is broadly consistent with expectations from circumplanetary disk simulations, which find that subdisks are truncated at $\sim 1/3 R_{\text{Hill}}$ as a result of the gravitational influence of the host star (Shabram & Boley 2013). For GSC 6214-210 B, this corresponds to a radius of ≈ 19 AU. Interestingly, the free-floating brown dwarf OTS 44 in Chamaeleon I has a similar mass ($\approx 12 M_{\text{Jup}}$) and accretion rate ($\sim 8 \times 10^{-12} M_\odot \text{ yr}^{-1}$) to GSC 6214-210 B, but possesses a significantly more massive disk of $\sim 30 M_\oplus$ and is consistent with having a spatial extent out to ~ 100 AU (Joergens et al. 2013). These differences could be caused by disk evolution owing to the different ages of these objects (~ 2 Myr versus 5–10 Myr), environmental influences from the nearby host star GSC 6214-210 A, natural variations in the physical properties of circumsubstellar disks, and/or differing formation mechanisms. It is also possible, though more speculative, that GSC 6214-210 B originally formed closer in and was dynamically scattered to a wide separation from an as-yet-undiscovered more massive companion. In this scenario, GSC 6214-210 B's disk could have been truncated, explaining its hot, inner component but low overall mass. We note that it is possible the disk may be very small ($\lesssim 0.4$ AU) and optically thick given the brightness temperature limit of <0.02 K, but that would require long-term stability of the disk in the face of short viscous timescales. Ultimately, the growing population of planetary-mass companions being found at hundreds of AU (Kraus et al. 2014) combined with ALMA's unprecedented sensitivity and spatial resolution will make it possible to explore these effects for larger samples of

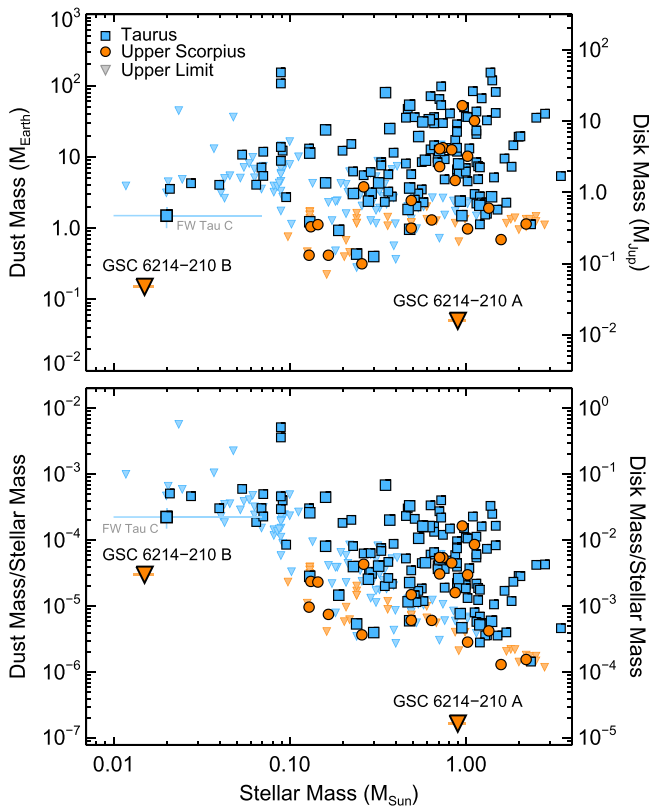


Figure 3. Top: sub-millimeter/millimeter dust mass measurements as a function of stellar mass for the ≈ 2 Myr Taurus (blue) and ≈ 5 – 10 Myr USco (orange) star-forming regions. Triangles denote 3σ upper limits. Our ALMA constraints for GSC 6214-210 A and B are over an order of magnitude lower than for most previous surveys in these regions. Taurus data are from Andrews et al. (2013) and Akeson & Jensen (2014); USco data are from Mathews et al. (2012) and Carpenter et al. (2014). Dust masses from Andrews et al. are derived from their $890 \mu\text{m}$ flux density measurements and dust temperature–stellar luminosity scaling with a lower boundary of 10 K adopted for the lowest-luminosity brown dwarfs in their sample. Ordinates on the right-hand axis denote total disk masses assuming an interstellar-like 100:1 gas-to-dust ratio. For comparison, the dust mass measurement of FW Tau C from Kraus et al. (2015) is labeled. Bottom: similar to the upper panel, but showing dust mass to stellar mass ratio (and total disk mass to stellar mass ratio) as a function of stellar mass. In terms of mass ratio, our non-detection of GSC 6214-210 B’s disk is not particularly unusual.

free-floating and bound planetary-mass objects spanning ages of 1–10 Myr.

In Figure 3 we compare our ALMA constraints to previous sub-millimeter/millimeter surveys in the Taurus and USco star-forming regions. Our upper limit for GSC 6214-210 A indicates there is a wide range of outcomes for protoplanetary disks around Sun-like stars in USco. Larger programs by Mathews et al. (2012) and Carpenter et al. (2014) found disk masses in excess of $10 M_{\text{Jup}}$, implying a spread of over three orders of magnitude in disk mass when taking into account our non-detection. Indeed, if the primary star GSC 6214-210 A harbors a disk, it must be at most a putative 0.0015% of the host star mass—much lower than the median disk-to-star mass ratio of $\sim 0.3\%$ found at younger ages by Andrews et al. (2013). Altogether it is clear that giant planet formation has ceased in this system.

Similarly, there is not enough dust in GSC 6214-210 B’s disk for gas giant “moons” to form, but we cannot rule out future rocky moons with masses of $\approx 0.15 M_{\oplus}$ (≈ 12 lunar masses). Canup & Ward (2006) find that the shared mass ratio

of Jupiter, Saturn, and Uranus to the total mass of their regular moons ($\sim 10^4$) can be explained by a balance between inflowing material into their circum-planetary disks, which provides the raw material for creating new moons, and satellite loss through orbit decay. In this scenario the current regular moons around these gas giants are simply the last generation of those formed from their subdisks. The current dust content of GSC 6214-210 B is a factor of at least three lower than this planet-moon mass ratio, so if this phenomenon is universal then any moons already formed or in the process of forming in this system will probably be the last ones.

Assuming a steady-state accretion rate, the lifetime of GSC 6214-210 B’s disk can be estimated from its accretion rate ($10^{-10.8} M_{\odot} \text{yr}^{-1}$; Zhou et al. 2014) and disk mass constraint. At most, accretion will continue for another ~ 3 Myr, though the fractional gain in planet mass is only $< 0.4\%$. The GSC 6214-210 AB system therefore appears to be in its last stages of assembly, with giant planet formation having ceased around the primary star and moon formation probably in its final stages around the companion.

We are grateful to the referee for helpful comments, Jonathan Swift for productive discussions about pursuing this idea, and Vanessa Bailey for providing zero point flux densities for MMT and LBT filters. This paper makes use of the following ALMA data: ADS/JAO.ALMA#2013.1.00487.S. ALMA is a partnership of ESO (representing its member states), NSF (USA), and NINS (Japan), together with NRC (Canada) and NSC and ASIAA (Taiwan), in cooperation with the Republic of Chile. The Joint ALMA Observatory is operated by ESO, AUI/NRAO, and NAOJ. The National Radio Astronomy Observatory is a facility of the National Science Foundation operated under cooperative agreement by Associated Universities, Inc. We utilized data products from the 2MASS, which is a joint project of the University of Massachusetts and the Infrared Processing and Analysis Center/California Institute of Technology, funded by the National Aeronautics and Space Administration and the National Science Foundation. NASA’s Astrophysics Data System Bibliographic Services together with the VizieR catalog access tool and SIMBAD database operated at CDS, Strasbourg, France, were invaluable resources for this work.

Facility: ALMA

REFERENCES

- Akeson, R. L., & Jensen, E. L. N. 2014, *ApJ*, 784, 62
 Alibert, Y., Mordasini, C., Benz, W., & Winisdoerffer, C. 2005, *A&A*, 434, 343
 Allard, F., Homeier, D., & Freytag, B. 2010, arXiv:1011.5405
 Andrews, S. M., Rosenfeld, K. A., Kraus, A. L., & Wilner, D. J. 2013, *ApJ*, 771, 129
 Ayliffe, B. A., & Bate, M. R. 2009, *MNRAS*, 397, 657
 Bailey, V., Hinz, P. M., Currie, T., et al. 2013, *ApJ*, 767, 31
 Baraffe, I., Chabrier, G., Allard, F., & Hauschildt, P. H. 1998, *A&A*, 337, 403
 Bate, M. R. 2009, *MNRAS*, 392, 590
 Beckwith, S. V. W., Sargent, A. I., Chini, R. S., & Guesten, R. 1990, *AJ*, 99, 924
 Boss, A. P. 1997, *Sci*, 276, 1836
 Bowler, B. P., Liu, M. C., Kraus, A. L., & Mann, A. W. 2014, *ApJ*, 784, 65
 Bowler, B. P., Liu, M. C., Kraus, A. L., Mann, A. W., & Ireland, M. J. 2011, *ApJ*, 743, 148
 Brandt, T. D., McElwain, M. W., Turner, E. L., et al. 2014, *ApJ*, 794, 159
 Canup, R. M., & Ward, W. R. 2002, *AJ*, 124, 3404
 Canup, R. M., & Ward, W. R. 2006, *Natur*, 441, 834
 Carpenter, J. M., Ricci, L., & Isella, A. 2014, *ApJ*, 787, 42

- Heller, R., Williams, D., Kipping, D., et al. 2014, *AsBio*, **14**, 798
- Hildebrand, R. H. 1983, *QJRAS*, **24**, 267
- Ireland, M. J., Kraus, A., Martinache, F., Law, N., & Hillenbrand, L. A. 2011, *ApJ*, **726**, 113
- Isella, A., Chandler, C. J., Carpenter, J. M., Pérez, L. M., & Ricci, L. 2014, *ApJ*, **788**, 129
- Joergens, V., Bonnefoy, M., Liu, Y., et al. 2013, *A&A*, **558**, L7
- Kalas, P., Graham, J. R., Chiang, E., et al. 2008, *Sci*, **322**, 1345
- Kenworthy, M. A., & Mamajek, E. E. 2015, *ApJ*, **800**, 126
- Kraus, A. L., Andrews, S. M., Bowler, B. P., et al. 2015, *ApJ*, **798**, L23
- Kraus, A. L., & Ireland, M. J. 2012, *ApJ*, **745**, 5
- Kraus, A. L., Ireland, M. J., cieza, L. A., et al. 2014, *ApJ*, **781**, 20
- Kraus, A. L., Ireland, M. J., Martinache, F., & Lloyd, J. P. 2008, *ApJ*, **679**, 762
- Kuzuhara, M., Tamura, M., Kudo, T., et al. 2013, *ApJ*, **774**, 11
- Lachapelle, F.-R., LaFreniere, D., Gagné, J., et al. 2015, *ApJ*, **802**, 1
- Lagrange, A.-M., Gratadour, D., Chauvin, G., et al. 2009, *A&A*, **493**, L21
- Lubow, S. H., Seibert, M., & Artymowicz, P. 1999, *ApJ*, **526**, 1001
- Luhman, K. L., & Mamajek, E. E. 2012, *ApJ*, **758**, 31
- Mamajek, E. E., Quillen, A. C., Pecaut, M. J., et al. 2012, *ApJ*, **143**, 72
- Marley, M. S., Fortney, J. J., Hubickyj, O., Bodenheimer, P., & Lissauer, J. J. 2007, *ApJ*, **655**, 541
- Marois, C., Macintosh, B., Barman, T., et al. 2008, *Sci*, **322**, 1348
- Marois, C., Zuckerman, B., Konopacky, Q. M., Macintosh, B., & Barman, T. 2010, *Natur*, **468**, 1080
- Martin, R. G., & Lubow, S. H. 2011, *MNRAS*, **413**, 1447
- Mathews, G. S., Williams, J. P., Menard, F., et al. 2012, *ApJ*, **745**, 23
- Pecaut, M. J., Mamajek, E. E., & Bubar, E. J. 2012, *ApJ*, **746**, 154
- Pollack, J. B., Hubickyj, O., Bodenheimer, P., et al. 1996, *Icar*, **124**, 62
- Preibisch, T., Guenther, E., Zinnecker, H., et al. 1998, *A&A*, **333**, 619
- Quanz, S. P., Amara, A., Meyer, M. R., et al. 2013, *ApJ*, **766**, L1
- Quillen, A. C., & Trilling, D. E. 1998, *ApJ*, **508**, 707
- Rameau, J., Chavin, G., Lagrange, A.-M., et al. 2013, *ApJ*, **779**, L26
- Ricci, L., Testi, L., Natta, A., et al. 2014, *ApJ*, **791**, 20
- Shabram, M., & Boley, A. C. 2013, *ApJ*, **767**, 63
- Vorobyov, E. I., & Basu, S. 2010, *ApJ*, **714**, L133
- Ward, W. R., & Canup, R. M. 2010, *AJ*, **140**, 1168
- Zhou, Y., Herczeg, G. J., Kraus, A. L., Metchev, S., & Cruz, K. L. 2014, *ApJ*, **783**, L17
- Zhu, Z. 2015, *ApJ*, **799**, 16